

# 1 **The secretory fate of flavivirus NS1 in mosquito cells is influenced by the** 2 **caveolin binding domain**

3 Romel Rosales Ramirez<sup>1</sup> and Juan E. Ludert<sup>1\*</sup>

4 <sup>1</sup> Department of Infectomics and Molecular Pathogenesis, Center for Research and Advanced  
5 Studies (CINVESTAV-IPN) Mexico City, Mexico.

6

7 \*Corresponding author

8 E-mail: [jludert@cinvestav.mx](mailto:jludert@cinvestav.mx)

9

## 10 **Keywords:**

11 Dengue; Zika; flavivirus; NS1; caveolin; viral protein trafficking; unconventional secretion;  
12 mosquito cells.

13

## 14 **ABSTRACT**

15 Flaviviruses of major medical importance worldwide such as dengue (DENV), Zika (ZIKV), and  
16 yellow fever (YFV) viruses are transmitted by mosquitoes *Aedes sp.* The non-structural protein  
17 1 (NS1) of these flaviviruses is secreted from the infected cells using different secretion routes  
18 depending on the cell and virus nature. The NS1 of DENV and ZIKV contain in the hydrophobic  
19 region a conserved caveolin binding domain (CBD) ( $\Phi XX\Phi XXXX\Phi$ ), which is not conserved in  
20 YFV NS1. To ascertain the role of the CBD in the secretory route followed by flavivirus NS1,  
21 expression vectors for the NS1 of DENV2, ZIKV and YFV were constructed. Using site-directed  
22 mutagenesis, substitutions were made in the aromatic residues within CBD; in addition, the full  
23 domain was replaced by those of other flaviviruses, creating chimeras in the CBD of NS1.  
24 Substitutions of the aromatic residues to Ala or Thr, or CBD chimeras, results in increased  
25 sensitivity of NS1 secretion to brefeldin A treatment, indicating a change to a classical secretion  
26 pathway. Likewise, the insertion of the DENV/ZIKV CBD into the recombinant *Gaussia-*

27 Luciferase results in a loss of sensitivity to BFA treatment, in luciferase secretion. These results  
28 suggest that the CBD sequence is a molecular determinant for the unconventional secretory  
29 route followed by DENV and ZIKV NS1 in mosquito cells. However, the cellular components that  
30 recognize the CBD in the NS1 of DENV and ZIKV and redirect them to an unconventional route  
31 and if this secretion route confers unique functions to NS1 within the vector mosquito are aspects  
32 currently unknown.

33

34

## 35 **Importance**

36 Flaviviruses are an important cause of mosquito borne diseases to humans. We have previously  
37 demonstrated that the non-structural protein 1 from dengue and zika virus are secreted efficiently  
38 from mosquito cells using an unconventional route, that depends on caveolin and molecular  
39 chaperones. In this work, we show evidence indicating that a caveolin binding domain, well  
40 conserved and exposed in dengue and Zika virus NS1, but absent in other flaviviruses such as  
41 yellow fever virus or West Nile virus, is important in determining the unconventional secretion  
42 pathway followed by dengue and zika virus NS1 in mosquito cells. The unique secretory pathway  
43 followed by NS1 in mosquito cells may result in distinctive viral-cellular protein associations  
44 required to facilitate viral infection in the mosquito vector. To identify viral and cellular elements  
45 that could disturb the traffic of dengue and Zika virus NS1 may be important to design of  
46 strategies for vector control.

47

## 48 **INTRODUCTION**

49 The *Flaviviridae* family includes many significant viral human pathogens, including yellow fever  
50 virus (YFV), dengue virus (DENV), Zika virus (ZIKV), West Nile virus (WNV), Japanese  
51 encephalitis virus (JEV), and tick-borne encephalitic virus (TBEV). The flavivirus virion particles  
52 are small (~50 nm) and contain a single-stranded positive RNA genome of nearly 11,000 bases  
53 in length (1). DENV is the only flavivirus with four serotypes (DENV1-4) and infection with any  
54 of them can cause dengue fever or severe dengue. DENV, ZIKV and YFV are transmitted by

55 *Aedes* mosquitoes and circulate in tropical and sub-tropical regions of the globe (2). There are  
56 several environmental, demographic and eco-logical reasons to believe that either novel or  
57 known flaviviruses will continue to emerge. In this respect, the success of vaccination against  
58 YFV has been temperate by difficulties encountered when vaccination was launched against  
59 DENV(3). In particular, the presence of four DENV serotypes has complicated vaccine design  
60 because incomplete protection against one serotype may influence the disease outcome, once  
61 infection is established by a distinct serotype, through a process referred to as antibody-  
62 mediated disease enhancement (4).

63 The flavivirus genome encodes only one open reading frame that is translated as one large  
64 polyprotein. The polyprotein is then cleaved by host and viral proteases to release individual  
65 viral proteins. The genome of most flavivirus encodes for three structural (C, E, prM/M) and  
66 seven non-structural (NS) (NS1, NS2A, NS2B, NS3, NS4A, NS4B, NS5) proteins (5). In DENV,  
67 the NS1 protein act as an scaffolding protein that anchors the replication complex to the ER  
68 membrane and interacts physically with NS4B (6). The NS1 protein is a 352-amino-acid  
69 polypeptide with a molecular weight of 46–55 kDa, depending on its glycosylation status. The  
70 NS1 protein exists in multiple oligomeric forms and is found in different cellular locations: a cell  
71 membrane-bound form in association with virus-induced intracellular vesicular compartments,  
72 on the cell surface and as a soluble secreted hexameric lipoparticle (6). The NS1 monomeric  
73 form rapidly dimerizes in the endoplasmic reticulum (ER), then three dimeric forms of NS1  
74 arrange to form an hexamer (7). The hexameric form of NS1 shows an open barrel form filled  
75 with lipids and cholesterol which resemble the lipid composition of the HDL particle (8). NS1  
76 associated pathogenesis, comprising several diverse mechanisms, in the vertebrate host has  
77 been described (9, 10). However, the possible NS1 pathogenic effects within the mosquito vector  
78 are a matter of study and are not been well understood yet (11).

79

80 In a previous work, DENV and ZIKV NS1 secretion in infected mosquito cells was associated to  
81 a caveolin-1 (CAV-1) dependent, unconventional secretory pathway that bypasses the Golgi-  
82 complex (12, 13). In contrast, YFV NS1 is secreted in both vertebrate and mosquito cells using  
83 Golgi-dependent, classical secretory pathway (13, 14). Furthermore, it was determine that NS1  
84 secretion in mosquito cells is dependent on the caveolin chaperone complex (CCC) (13). The

85 interaction of proteins with CAV-1, which seems to be important in the recruitment of proteins to  
86 the caveolar domains and, therefore, in the formation of microenvironments rich in interactive  
87 signaling molecules, is believed to be mediated through the interaction of an N- 20 amino acid  
88 terminal region in the caveolin molecule, known as the caveolin scaffolding domain, and the  
89 CBD present in the likely caveolin binding proteins (15–17). The CBD is defined as a sequence  
90 of three or four aromatic residues separated by unspecified amino acids ( $\Phi$ X $\Phi$ XXXX $\Phi$ ,  
91  $\Phi$ XXXX $\Phi$ XX $\Phi$  or  $\Phi$ X $\Phi$ XXXX $\Phi$ XX $\Phi$ , where  $\Phi$  is any aromatic amino acid) (15). The NS1 of all 4  
92 DENV serotypes and ZIKV present a well conserved and exposed caveolin-binding domain  
93 (FXXFXXXXW) (12), which is absent in others mosquito borne flaviviruses such as YFV, WNV  
94 and JEV. The DENV and ZIKV NS1 CDB is located in the connector subdomain, in the so-called  
95 “butter fingers”, a hydrophobic region which creates a protrusion with a hydrophobic surface,  
96 that in the dimer is in close contact with the lipid bilayer and in the hexamer is in contact with the  
97 lipids in the center (18).

98 The previous observation that DENV and ZIKV associate with CAV-1 and the CCC, and are  
99 secreted bypassing the Golgi-complex while the YFV NS1 do not show such associations and  
100 is secreted by a classical secretory route (12, 13), indicate that the association of DENV and  
101 ZIKV NS1 with the CCC, and the use of an unconventional secretory route, may respond to the  
102 presence of the CBD. Therefore, in this work, we examined in more detail the relationship  
103 between the CBD sequence in the flavivirus NS1 and its secretion pathway. By using site point  
104 mutations in aromatics residues and the generation of chimeras, data was obtained indicating  
105 that indeed the unconventional secretion route followed by DENV and ZIKV NS1 in mosquito  
106 cells is influenced by the CDB. This work brings new knowledge about how the secretory  
107 machinery in mosquito cells senses sequences in proteins and directs them to its secretion  
108 pathway.

109

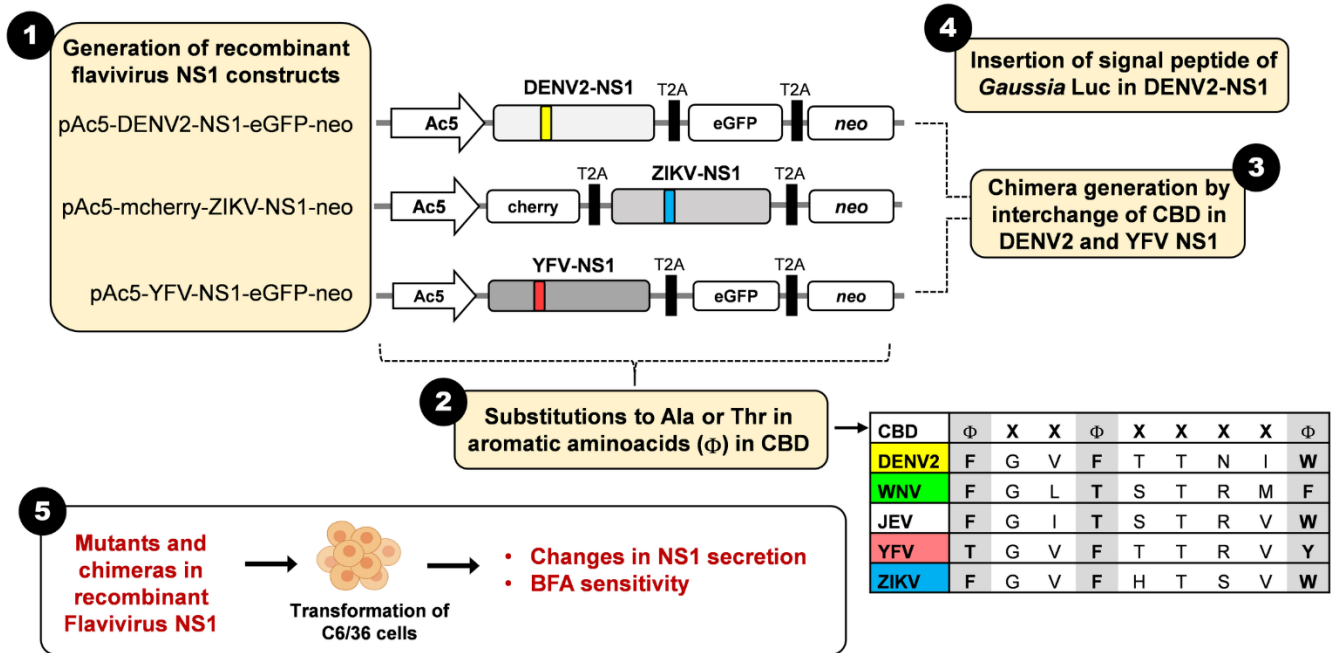
## 110 **RESULTS**

111 To determine whether the presence of CBD in the NS1 sequence of DENV or ZIKV influences  
112 the secretion path of NS1 in mosquito cells, first plasmids with the recombinant DENV, ZIKV and  
113 well as YFV, for comparison, interest were generated. In addition, to site-directed mutants,

114 clones with full substitution of the CBD between different NS1s and NS1 chimeras with *Gau*-Luc  
 115 were generated. Figure 1 shows the general experimental scheme followed by in this work and  
 116 Table 1 the list of all primers used.

117

118



119

120 **Fig 1. Schematic representation of the overall site directed mutagenesis strategy. 1. Generation**  
 121 **of recombinant flavivirus NS1.** The details for the construction of recombinants NS1 are in Materials  
 122 and Methods. Each construct was used as template for site directed mutagenesis. Actin5C promoter;  
 123 cherry, red fluorescent protein; eGFP, eukaryotic green fluorescent protein; neo, resistance to neomycin,  
 124 kanamycin and G418, each gene separated by a T2A peptide. Yellow and blue; DENV and ZIKV NS1  
 125 CBD sequences; red; YFV NS1 incomplete CBD. **2. Substitutions of aromatic residues in CBD to Ala**  
 126 **or Thr.** CBD sequences of flaviviruses used in this manuscript. Note that WNV, and ZIKV present  
 127 aromatic residues in all 3 positions. A few substitutions produce another flavivirus phenotypes in CBD  
 128 sequence. **3. Chimera generation by interchange of CBD in DENV2 and YFV NS1.** The complete  
 129 sequence of DENV2 CBD was substituted by the ZIKV or YFV CBD sequences. The complete sequence  
 130 of YFV CBD was substituted by the DENV2 or WNV CBD sequences. **4. Insertion of signal peptide of**  
 131 ***Gaussia* Luc in DENV2-NS1.** This insertion was introduced only in the DENV2-NS1 construct. **5.**  
 132 **General experimental strategy with constructs.** All mutations, insertions and chimera constructions  
 133 were transfected in C6/36 cells and NS1 secretion to the supernatants in cells treated or not with BFA  
 134 determined by ELISA.

135

136

Primer	Sequence (5'→ 3')	Desired Mutation
<b>Single point mutations in pAc5-DENV2-NS1-eGFP-neo</b>		
D_F188A_F	AGACTATGGCGCCGGAGTATTCACC	F188A
D_F188A_R	TCAACTTCCAACGAATTC	
D_F188T_F	AGACTATGGCACAGGAGTATTCACC	F188T
D_F188T_R	TCAACTTCCAACGAATTC	
D_F191A_F	CTTTGGAGTAGCCACCACCAATATATG	F191A
D_F191A_R	CCATAGTCTTCAACTTCC	
D_F191T_F	CTTTGGAGTAACCACCACCAATATATG	F191T
D_F191T_R	CCATAGTCTTCAACTTCC	
D_W196A_F	CACCAATATAGCGCTAAAATTGAAAGAAAAACAG	W196A
D_W196A_R	GTGAATACTCCAAAGCCATAG	
D_W196T_F	CACCAATATAACGCTAAAATTGAAAGAAAAAC	W196T
D_W196T_R	GTGAATACTCCAAAGCCATAG	
<b>Insertion of signal peptide (GLuc) in N-terminal of DENV2-NS1</b>		
D_SSLuc_F	ATCTGCATCGCTGTGGCCGAGGCCGGATCACGCAGCACCTC AC	Insertion of GVKVLFALICIAVAE A in 15-16 bp
D_SSLuc_R	CAGGGCAAACAGAACTTTGACTCCCATGGTGGCGGTACCCC G	
<b>Single point mutations in pAc5-mCherry-ZIKV-NS1-neo</b>		
Z_F159A_F	GGATCATGGGGCCGGGGTATTCC	F159A
Z_F159A_R	TCCACAAGAAAGCTGTTC	
Z_F159T_F	GGATCATGGGACAGGGGTATTCC	F159T
Z_F159T_R	TCCACAAGAAAGCTGTTC	
Z_F162A_F	GTTCGGGGTAGCCACACTAGTG	F162A

Z_F162A_R	CCATGATCCTCCACAAGAAAG	
Z_F162T_F	GTTTCGGGGTAACACACACTAGTGTC	F162T
Z_F162T_R	CCATGATCCTCCACAAGAAAG	
Z_W167A_F	CACTAGTGTCGCCCTCAAGGTTAGAGAAGATTATTCATTAG	W167A
Z_W167A_R	TGGAATACCCCGAACCCA	
Z_W167T_F	CACTAGTGTCACACTCAAGGTTAGAGAAGATTATTC	W167T
Z_W167T_R	TGGAATACCCCGAACCCA	
<b>Single point mutations in pAc5-YFV-NS1-eGFP-neo</b>		
Y_T161A_F	AGAGTTTGGGGCCGGAGTGTTCCAC	T161A
Y_T161A_R	TCTATCTGGAAGGAATTCCAC	
Y_T161F_F	AGAGTTTGGGTTTGGAGTGTTCCAC	T161F
Y_T161F_R	TCTATCTGGAAGGAATTCC	
Y_F164A_F	GACAGGAGTGGCCACCACCCGAG	F164A
Y_F164A_R	CCAAACTCTTCTATCTGGAAG	
Y_F164T_F	GACAGGAGTGACAACCACCCGAG	F164T
Y_F164T_R	CCAAACTCTTCTATCTGGAAG	
Y_Y169A_F	CACCCGAGTGGCCATGGATGCAG	Y169A
Y_Y169A_R	GTGAACACTCCTGTCCCA	
Y_Y169T_F	CACCCGAGTGACAATGGATGCAGTCTTTG	Y169T
Y_Y169T_R	GTGAACACTCCTGTCCCA	
<b>Insertion of Flavivirus CBD in pAc5-mCherry-Gaussia-Luciferase-neo</b>		
InsertCBD-D2_F	CACCAATATATGGAACGAAGACTTCAACATCGTGG	Insertion of DENV2-CBD (FGVFTTNIW) between 22-23 residues
InsertCBD-D2_R	GTGAATACTCCAAAGTTCTCGGTGGGCTTGCC	

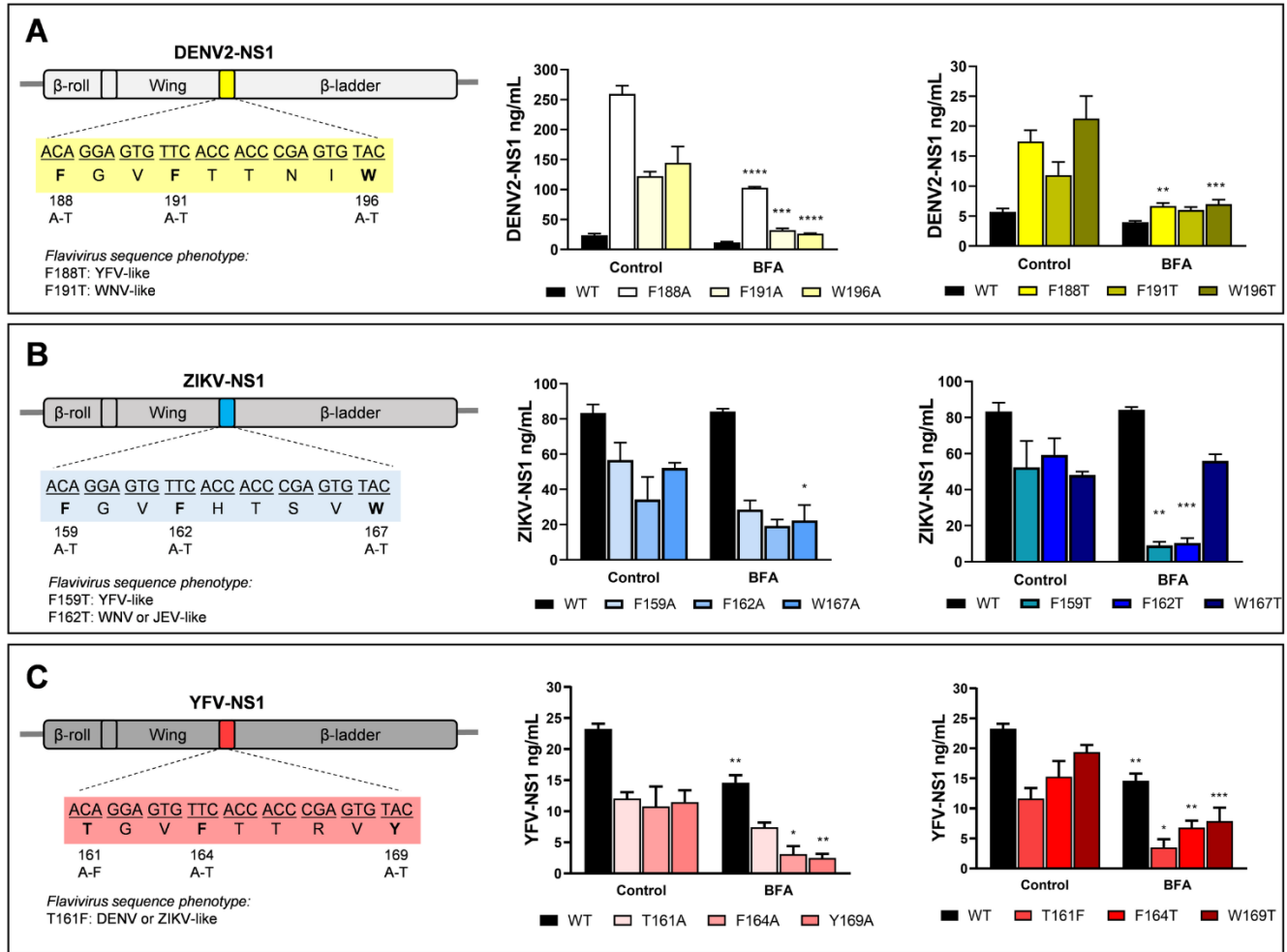
InserCBD-YFV_F	CACCCGAGTGTACAACGAAGACTTCAACATCGTGG	Insertion of YFV-CBD (TGVFTTRVY) between 22-23 residues
InserCBD-YFV_R	GTGAACACTCCTGTGTTCTCGGTGGGCTTGGC	
<b>Chimeras of DENV2-NS1 with substitution of CBD</b>		
D_Chim-ZIKVCBD_F	CACTAGTGTCTGGCTAAAATTGAAAGAAAAACAGG	Substitution to ZIKV-CBD
D_Chim-ZIKVCBD_R	TGGAATACCCCGAAGCCATAGTCTTCAACTTC	
D_Chim-YFVCBD_F	CACCCGAGTGTACCTAAAATTGAAAGAAAAACAGG	Substitution to YFV-CBD
D_Chim-YFVCBD_R	GTGAACACTCCTGTGCCATAGTCTTCAACTTC	
<b>Chimeras of YFV-NS1 with substitution of CBD</b>		
Y_Chim-DENV2CBD_F	CACCAATATATGGATGGATGCAGTCTTTGAG	Substitution to DENV2-CBD
Y_Chim-DENV2CBD_R	GTGAATACTCCAAACCCAACTCTTCTATCTG	
Y_Chim-WNVCBD_F	CACTCGGATGTTTCATGGATGCAGTCTTTGAG	Substitution to WNV-CBD
Y_Chim-WNVCBD_R	CTGGTGAGACCAAACCCAACTCTTCTATCTG	

138

139 **Table 1.** List of primers used for the site directed mutagenesis. DENV CBD located between  
 140 574-600 bp (188-196 aa); ZIKV CBD located between 1336-1362 bp (159-167 aa) and YFV CBD  
 141 located between 493-519 bp (161-169 aa).

142





143

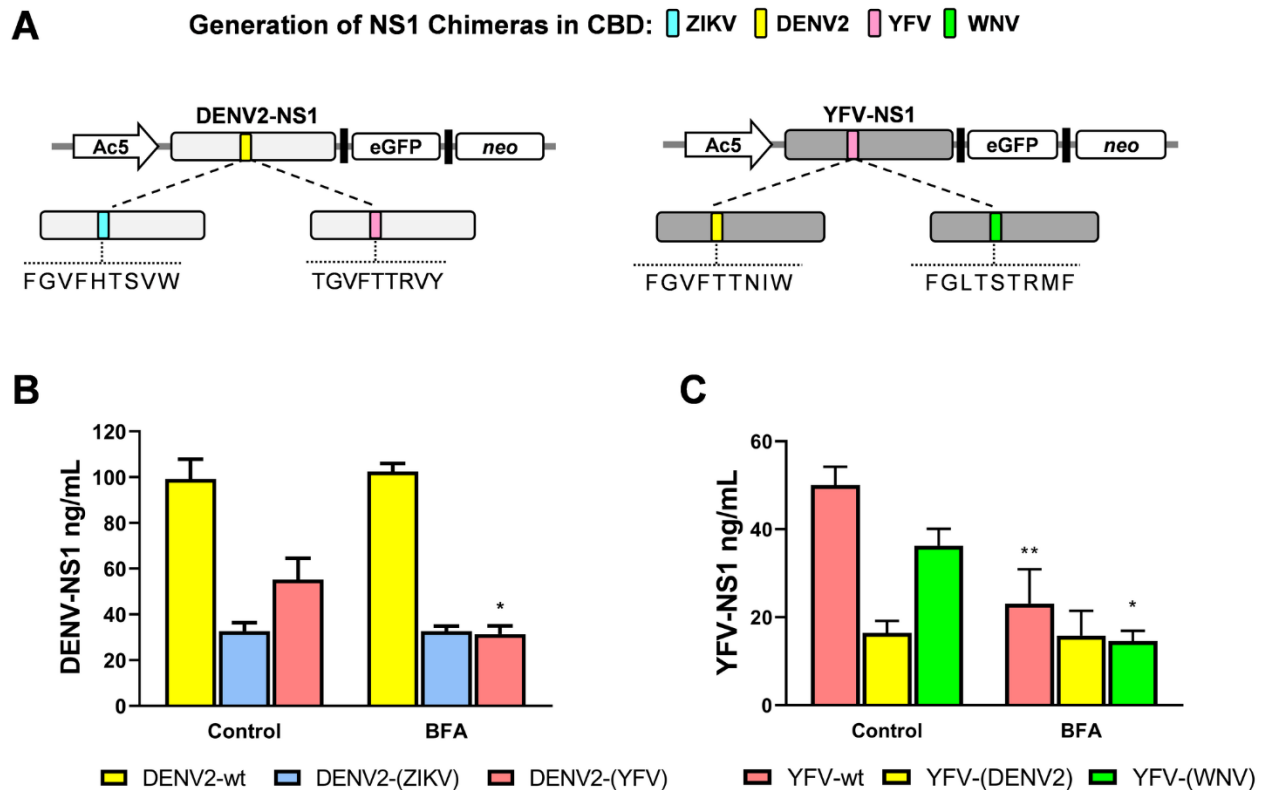
144 **Figure 2. Secretory phenotype of recombinant DENV (A), ZIKV (B) and YFV (C) NS1 mutated in the**  
 145 **CBD.** *Left panels*, schematic representation of the mutations introduced in each of the NS1 genes.  
 146 *Secretion mutated NS1 to Ala (central panels) and Thr or Phe (right panels) in C6/36 cells treated or not*  
 147 *with BFA. Twenty-four hours post-transfection, C6/36 cells were treated with DMSO (control) or with 25*  
 148 *μM BFA and the supernatants harvested after 48 h. Levels of secreted NS1 were measured by ELISA.*  
 149 *Data are mean of 3 independent experiments ± standard error; significant differences between controls and*  
 150 *BFA treatment are denoted by \* ( $p < 0.0001$ ).*

151

152 Aromatic positions in the DENV and ZIKV NS1 CBD were each change to Ala or Thr (Figure 1  
 153 and 2). Mutations to A were “non-sense”, but mutations F to T in the first aromatic position made  
 154 the sequence YFV-like, and in the second aromatic position, WNV and JEV-like (Figure 1 and  
 155 2). In turn, the A to F mutation in the first aromatic residue of YFV NS1 result in the restoration  
 156 of a full CBD. Mutations to both Ala or Thr in DENV NS1 resulted in a significant increase in the  
 157 amount of secreted NS1. Interestingly, all three A and T DENV NS1 mutants showed increased

158 secretion sensitivity to cell treatment with BFA, suggesting that the mutated DENV NS1 is at  
159 least partially secreted following a classical secretory pathway (Figure 2A). Results obtained  
160 with ZIKV NS1 mutants were less consistent; with increased NS1 secretion sensitivity to BFA  
161 cell treatment observed for only 3 of the 6 mutants constructed; that is mutants W167A and  
162 F159T and F162T, which convert them into a sequence similar to that of YFV and WNV (Figure  
163 2B). Finally, in the case of the introduced mutations to YFV NS1, which sought to make secretion  
164 less sensitive BFA treatment, no significant changes in BFA sensitivity were observed; even the  
165 T161F mutation that converts the sequence into a complete CBD does not produce resistance  
166 to BFA (Figure 2C). In view of the results obtained with the single point mutations, complete  
167 substitutions of the DENV and YFV NS1 CBD were made (Figure 3). The DENV NS1 CBD was  
168 replaced for the complete YFV NS1 sequence, and the ZIKV NS1 CBD, as control. The YFV  
169 NS1 sequence was replaced by the DENV NS1 CBD and the WNV sequence, as control (Figure  
170 3A). The results shown in Figure 3B indicate that the secretion of the DENV NS1 inserted with  
171 the YFV sequence, becomes sensitive to the treatment with BFA, while insensitivity to BFA is  
172 retained in the DENV NS1 with the ZIKV NS1 CBD. In addition, the insertion of the DENV NS1  
173 CBD into the YFV NS1 sequence, renders the YFV NS1 secretion insensitive to BFA, while  
174 sensitivity for BFA treatment is still observed for the YFV NS1 inserted with the WNV sequence  
175 (Figure 3C).

176



177

178 **Figure 3. Secretory phenotype of CBD-chimeras of flavivirus NS1.** **A.** Schematic representation of  
179 the chimeras generated from DENV (left) and YFV (right) NS1. Colors indicate the origin of the CBD. **B.**  
180 Secretion of DENV2-NS1 chimeras with ZIKV and YFV CBD. **C.** Secretion of YFV-NS1 chimeras with  
181 DENV and WNV CBD. Twenty-four hours post-transfection, C6/36 cells were treated with DMSO (control)  
182 or with 25  $\mu$ M BFA and the supernatants harvested after 48 h. Levels of secreted NS1 were measured  
183 by ELISA. Data are mean of at least 3 independent experiments  $\pm$  standard error; significant differences  
184 compared with controls are denoted by \* ( $p < 0.0001$ ).

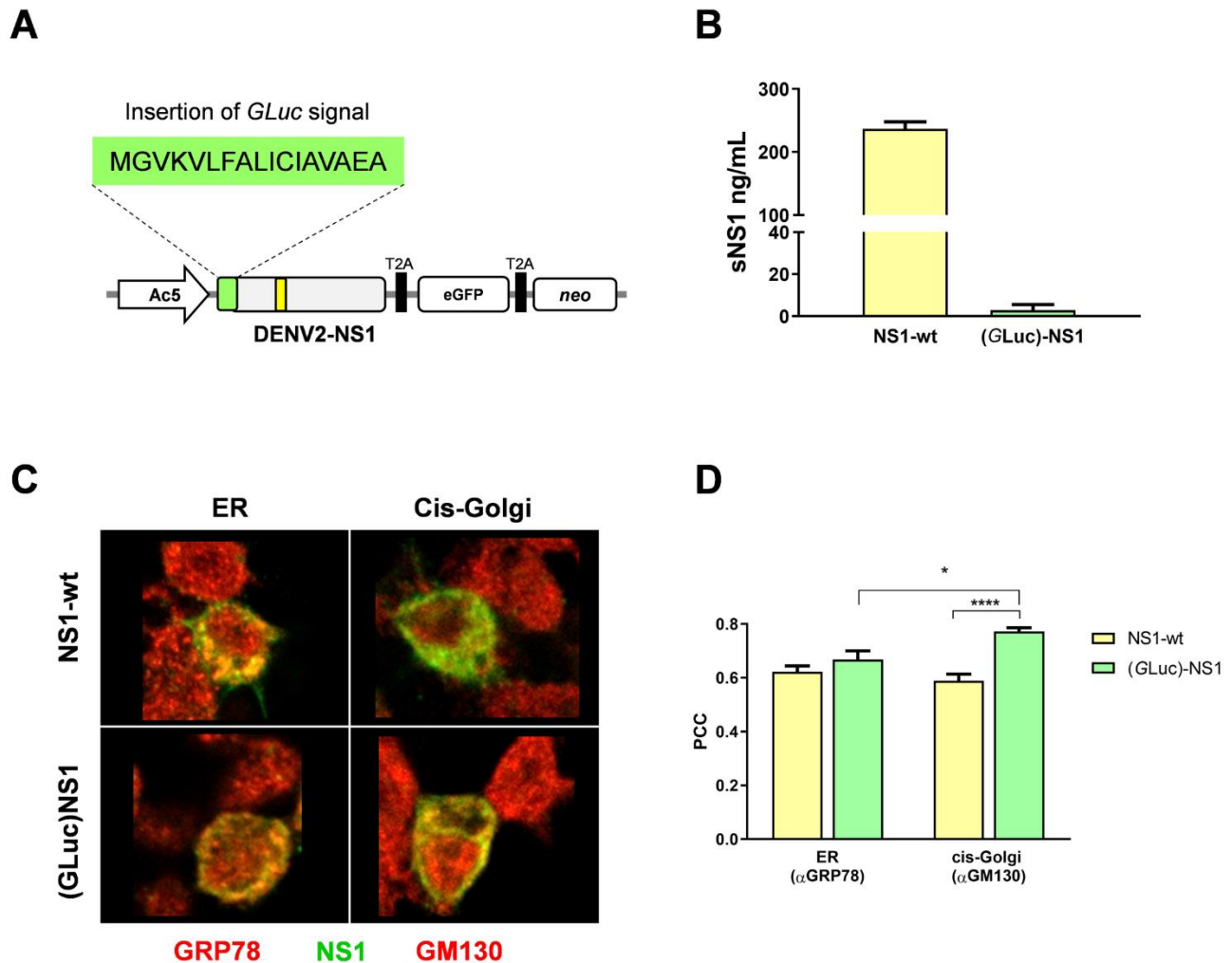
185

186

187 In an attempt to force the secretion of DENV NS1 to follow a conventional secretory route, even  
188 in the presence of the CBD, the secretion sequence of *Gaussia* Luciferase, a protein that in  
189 mosquito cells is secreted by a conventional secretory route, was inserted at the N-terminal end  
190 of DENV NS1. These 17 amino acids (MGVKVLFALICIAVAEA) were inserted into the N-terminal  
191 end of NS1, which lacks a signal sequence secretion, by site directed mutagenesis (Figure 4A).  
192 However, as shown in Figure 4B, the insertion decreased the secretion of NS1 by more than  
193 98%. Confocal microscopy analysis to determine where the GLuc-NS1 was being retained  
194 showed that the wild type protein was mostly located in the ER, while the (GLuc)-NS1 was

195 observed not only in the ER but also in the Golgi-complex (Figure 4C and D). These results  
196 suggest that although the mutant protein reached the Golgi apparatus, it was retained there and  
197 not secreted, possibly due to retrograde transport to ER.

198



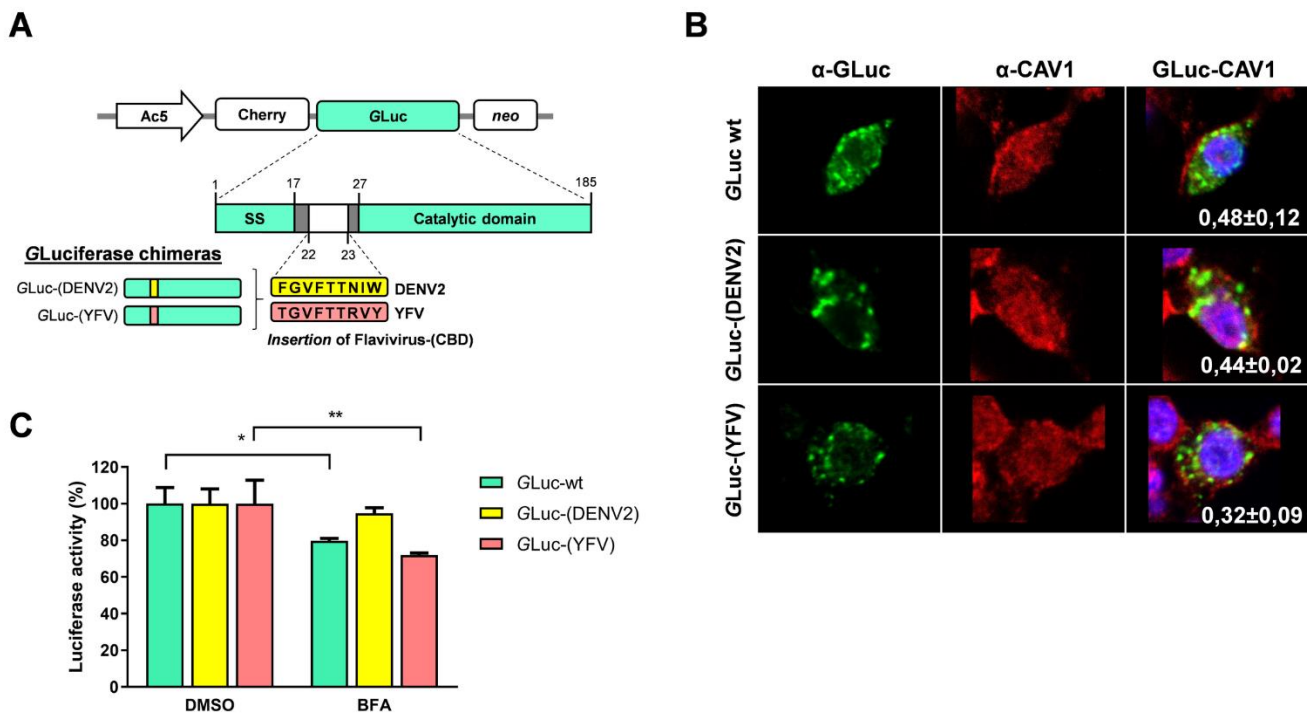
199

200 **Figure 4. Secretory phenotype of DENV2-NS1 after addition of the signal peptide of *Gaussia***  
201 **Luciferase.** **A.** Schematic representation of the construction obtained after insertion of the GLuc signal  
202 peptide in the N-terminal of recombinant DENV2-NS1. The sequence MGVKVLFALICIAVAEA was  
203 introduced by site directed mutagenesis as described in the methods section. **B.** Secretion of GLuc-NS1  
204 was measured in cells supernatants 48h post transfection. **C.** Co-localization between DENV2-NS1-wt  
205 or DENV2-GLuc-NS1 and ER (GRP78) and *cis*-Golgi (GM130) markers. Recombinants NS1 were  
206 transfected and 24hpt, cells were probed for NS1 (shown in green) and GRP78 or GM130 (shown in red).  
207 **D.** Pearson correlation coefficients (PCC) for organelle-NS1 were measured in at least 20 confocal  
208 independent images with 0.48  $\mu$ M laser sections. The bars represent means  $\pm$  standard error. Data was  
209 evaluated using the 2way ANOVA test and significant differences are denoted by \* ( $p \leq 0.05$ ).

210

211 Finally, to evaluate the effect that the presence of the DENV CBD may have on a protein  
 212 secreted by the classical route, a recombinant GLuc was constructed, into which the CBD of  
 213 DENV NS1 was inserted (Figure 5A). Upon examination of the GLuc sequence, it was decided  
 214 to insert the DENV CBD sequence, and that of YFV (as a negative control), between amino  
 215 acids 22-23. This region is located after the signal peptide and before the catalytic domain of the  
 216 luciferase and it is presumed to be exposed on the surface of the protein. Interestingly, the  
 217 presence of DENV CBD made the GLuc secretion significantly less sensitive to BFA treatment;  
 218 meanwhile the insertion of the equivalent YFV region did not produce any change (Figure 5C).  
 219 These results again suggest that the presence of a functional CBD will adjust the protein  
 220 secretory route, towards an unconventional route, in mosquito cells. Finally, co-localization  
 221 experiments between GLuc and CAV-1 were performed to assess whether the presence of CBD  
 222 would increase the interaction between Gluc and CAV-1. However, co-location analyzes,  
 223 quantified by PCC, showed no evidence of a significant increase in the interaction between both  
 224 proteins (Figure 5B).

225



226

227 **Figure 5. Secretory phenotype of *Gaussia* Luciferase after insertion of the DENV-NS1 CBD. A.**  
228 Schematic representation of the construction of GLuc with the inserted DENV-NS1 CBD. Color boxes  
229 indicate the origin of the CBD. Ac5: Actin5C promoter; Cherry: red fluorescent protein; neo: geneticin  
230 resistance; SS: signal secretion, catalytic domain of luciferase. **B.** Confocal microscopy analysis of GLuc  
231 chimeras with CAV-1. Recombinant GLuc chimeras were transfected and 24hpt, cells were probed for  
232 GLuc (shown in green) and CAV-1 (shown in red). The Pearson correlation coefficients (PCC) measured  
233 in at least 20 confocal independent images with 0.41  $\mu$ M laser sections for each condition are shown. **C.**  
234 Secretion of *Gaussia* Luciferase chimeras (DENV2 and YFV) in C6/36 cells treated for 48 hrs with BFA,  
235 or DMSO as control. Luciferase activity in control cells was taken as 100%. Experiments are based on at  
236 least three independent experiments with each chimera  $\pm$  standard error; significant differences  
237 compared with controls are denoted by \* ( $p < 0.0001$ ).

238

239

## 240 Discussion

241 The roles of NS1 in pathogenesis are associated to its presence in the extracellular and vascular  
242 space in the vertebrate host (9, 19, 20). However, the pathogenic effects within the mosquito  
243 vector are unknown. New findings have shown that flavivirus NS1 potently inhibits two important  
244 mosquito antiviral mechanisms (21). Although NS1 lacks a signal secretion in the N-terminal  
245 sequence, in vertebrate cells it follows a classical secretion pathway through Golgi to reach the  
246 extracellular space. In mosquito cells, an unconventional traffic route for secretion of DENV and  
247 ZIKV NS1 was observed, while in contrast, YFV NS1 seems to be secreted following the  
248 classical secretion route (11, 13). Given the presence of a conserved CBD in DENV and ZIKV  
249 NS1, but not in YFV NS1, a role for the CBD, as a molecular determinant, to direct the secretion  
250 fate within the *Aedes* endoplasmic reticulum architecture was proposed (13). Presumably, an  
251 active and exposed CBD in the hydrophobic region in the NS1 of flavivirus as DENV and ZIKV  
252 would facilitate the interaction with CAV-1 and directs the protein to an unconventional route in  
253 mosquito cells. In the present study, we employed a molecular genetic approach, using  
254 recombinant DENV, ZIK and YFV NS1s, to elucidate the role of the aromatic residues and the  
255 entire CBD in the secretory fate of flavivirus NS1 in mosquito cells.

256 By mutating any of the 3 aromatic amino acids of CBD in DENV2-NS1 that define the integrity  
257 of the CBD, the secretion of NS1 was changed from BFA cell treatment insensitive, to BFA  
258 sensitive, indicating that the mutants are now secreted, at least partially, following a classical  
259 secretory route through Golgi, as defined by BFA sensitivity (22–24). In addition, the DENV NS1

260 mutants, were secreted at significantly higher levels than the wild type protein. These changes  
261 in phenotype secretion suggest that the mutated DENV NS1 loses the ability to be recognized  
262 by CAV-1 or are recognized with less affinity, and therefore enter the route of classical secretion.  
263 Co-location analysis between point mutated DENV2 NS1 and CAV-1 showed no significant  
264 reduction in co-location levels (data not shown), a result which is compatible with only changes  
265 in affinity between NS1 and CAV-1. This observation is similar to previous observations where  
266 the mutation of several residues within CBD of a cholesterol transport-protein, abrogated the  
267 export of cholesterol but did not change the binding of the protein to cholesterol (25).

268 However, the single point mutations within the Zika NS1, resulted in variable secretion  
269 phenotypes regarding BFA sensitivity. While mutations to Ala in the third aromatic residue and  
270 to Thr in the first and second aromatic residue in CBD of ZIKV NS1 induce a sensitivity to BFA,  
271 other changes did not. The reasons for these differences with the DENV NS1 mutants are  
272 unknown, but differences in surface charges in the  $\beta$ -roll domain of the DENV and ZIKV NS1  
273 have been reported (26), and despite the full conservation of the aromatic residues, 3 of the 4  
274 amino acids found between the 2 and third aromatic residue are different, all of which may  
275 modulate the interaction between NS1 and CAV-1. In addition, the introduction of a T161F  
276 mutation to partially generate a CBD (aromatic amino acids in positions 1 and 2) into the YFV  
277 NS1, did not result in any change regarding BFA sensitivity, suggesting that the presence of a  
278 specific type of aromatic amino acid at the third position (like, Trp) and a complete CBD is  
279 required. All these results taken together suggest that single point mutations in DENV and ZIKV  
280 NS1 aromatic residues that disrupt the CBD result in changes in the traffic route of NS1 in  
281 mosquito cells.

282 Due to this behavior in the ZIKV and YFV NS1 single point mutants, we generated NS1 mutants  
283 where the complete CBD was exchanged. The DENV NS1 CBD was replaced by the YFV  
284 sequence (BFA sensitive) and the ZIKV CBD (BFA insensitive), as control; likewise, into the YFV  
285 NS1 the DENV CBD (BFA insensitive) was introduced and as a negative control, the sequence  
286 corresponding to WNV CBD. In both cases the presence of a conserved CBD, rendered the  
287 secretion of NS1 insensitive to BFA cell treatment, suggesting a secretion path change.  
288 Therefore, the presence of the two Phe, and the Trp at the end, appears to be necessary to  
289 direct the NS1 protein to follow an unconventional route. This conclusion was reinforced by the

290 results obtained when the DENV CBD was introduced into the unrelated protein GLuc, which is  
291 secreted by the conventional secretory route. Surprisingly, when the DENV2 CBD was  
292 introduced into the recombinant GLuc, the secretion of GLuc gained insensitivity to BFA  
293 treatment, suggesting that it was now partially secreted by an unconventional secretion pathway.  
294 In the GLuc the CBD was introduced into an exposed area, and away the catalytic domain. This  
295 was an important consideration, since it has been described that the sole presence of a CBD, if  
296 not well exposed, does not guarantee that the protein will interact with CAV-1 (15, 27).

297 The results shown indicate that an active CBD is a molecular determinant guiding the secretion  
298 of DENV and ZIKV NS1 through an unconventional secretion pathway in mosquito cells. Yet, it  
299 is puzzling that the same sequence is not active in vertebrate cells, where the NS1 of these  
300 viruses is secreted via the ER-Golgi classical route (6, 12, 13). Unfortunately, the CAV-1 gene  
301 in *Aedes* mosquito have not been identify; however, docking simulations done with NS1 and  
302 CAV-1 from other insects, such as ticks (*Ixodes* sp., and *Sarcoptes* sp), showed a greater affinity  
303 of the DENV NS1 for these caveolins than for the human CAV-1 (data not shown). Thus, the  
304 mosquito cellular component acting as a sensor or recruiter for NS1 in could be the CAV-1 itself,  
305 although a role for cell architecture and other proteins, such as those of the Sec complex, cannot  
306 be discarded. The nearly complete abolition of secretion observed with the DENV NS1 modified  
307 with a secretion signal peptide, illustrates the complexity of the problem. Another interesting  
308 observation is that the CBD is fully conserved in DENV and ZIKV NS1, while incomplete in other  
309 flaviviruses such as YFV, JEV and WNV. Secretion of YFV NS1 have been observed in mosquito  
310 cells albeit a higher concentration was maintained as cell-associated rather than secreted into  
311 the extracellular milieu (28); moreover, no NS1 secretion is observed in WNV or JEV infected  
312 mosquito cells (29, 30). Thus, the presence of an active CBD and the recognition of NS1 by the  
313 mosquito caveolin may be crucial for NS1 secretion in the mosquito, and suggest unique roles  
314 for the DENV and ZIKV soluble NS1 in the mosquito (11, 21).

315 In summary, this work demonstrates that the sequence of PheXXPheXXXXTrp seems to play a  
316 role in determining that the unconventional secretory route of DENV and ZIKV NS1 in mosquito  
317 cells; resulting in interaction with CAV-1 and chaperones of the CCC. However, more research  
318 is needed to fully understand the viral and cellular factors that determine that the mosquito cell  
319 secretion machinery identify the CBD sequence and redirect the secretion pathway of NS1. Why



320 these dramatic differences exist in the organization of the components of the secretion pathway  
321 between mosquitoes and in vertebrate cells is still an enigma. It is worth mentioning that the  
322 functions of the soluble NS1 in the mosquito are unknown and should be clarified; but may  
323 include the facilitation of the propagation of viral particles and the modulation of innate immunity.  
324 Finally, the manipulation of the lipid and cholesterol system in the mosquito can become a new  
325 target to reduce the secretion of NS1 and a new strategy to block the spread of mosquito-borne  
326 flaviviruses.

327

328

## 329 **MATERIALS AND METHODS**

### 330 **Construction of recombinant flavivirus NS1 expression vectors and site directed** 331 **mutagenesis**

332 Ac5-STABLE2-neo was a gift from Rosa Barrio and James Sutherland (Addgene plasmid #  
333 32426) (31). This plasmid was engineered to express recombinant flavivirus NS1 protein in  
334 mosquito cells. DENV2 NS1 (New Guinea C strain) gene was obtained from mammalian  
335 expression plasmid kindly donated by Dr. Ana Sesma (Icahn School of Medicine at Mount Sinai,  
336 New York). DENV2 NS1 was PCR-amplified using the following designed primers with directed  
337 cloning sites (underlined): *Forward primer-KpnI* (5'-  
338 GCTAGGTACCGCCACCATGGGATCACGCAGCACCTCACTGTCTGTG-3') and *reverse-*  
339 *primer-NotI* (5'-CTTCGCGCGGCCGCGGATCAGCTGTGACCAAGGAGTTGACCAAATTC-3').  
340 DENV2-NS1 KpnI-NotI cassette was cloned into pAc5-STABLE2-Neo, generating the pAc5-  
341 (DENV2) NS1-GFP-Neo vector, under the promoter Actin5C (from *Drosophila melanogaster*)  
342 reported to be efficient in insect cells lines (31–33). The T2A peptide sequence derived from  
343 *Thosea asigna* (EGRGSLTCDVEENPGP) allowed multicistronic processing and the  
344 neomycin resistance gene (NeoR) confers resistance to G418 allowing stable mosquito cell  
345 lines.

346 The NS1 sequence from ZIKV (Mexican isolate, Asiatic linkage) and YFV NS1 (Brazilian yellow  
347 fever virus isolate) were synthesized *de novo* (GenScript, Piscataway, NJ). The synthetic ZIKV  
348 NS1 gene (GenBank accession number KY631493.1) was ligated as a XbaI/HindIII fragment

349 into the similarly digested Ac5-stable2 expression cassette generating the pAc5–mCherry-  
350 (ZIKV)NS1-Neo vector. The synthetic YFV NS1 gene (GenBank accession number  
351 MH018093.1) was ligated as a KpnI/NotI fragment into the similarly digested Ac5-stable2  
352 expression cassette generating the pAc5–(YFV)NS1-GFP-Neo vector.

353 The secretion signal from *Gaussia* Luciferase (GVKVLFALICIAVAEA) was inserted in the N-  
354 terminal sequence of DENV2-NS1 using designed primers between 15-16 nucleotide. Aromatic  
355 residues (Phe/Trp/Tyr) in the caveolin binding domain (CBD) within flavivirus NS1 plasmids were  
356 substituted to Ala or Thr with primers listed in Table 1 To evaluate the effect of complete changes  
357 in the CBD in flavivirus NS1 sequence, we substituted the CBD from DENV2-NS1 to the CBD of  
358 ZIKV (TTCGGGGTATTCCACACTAGTGTCTGG), or the corresponding YFV sequence  
359 (ACAGGAGTGTTCCACCACCCGAGTGTAC). These substitutions produced chimeras named  
360 DENV2-(ZIKV) and DENV2-(YFV), respectively. The CBD from YFV-NS1 construct was  
361 substituted to the CBD of DENV2 (TTTGGAGTATTCACCACCAATATATGG) or WNV  
362 (TTTGGTCTCACCAGCACTCGGATGTTC). These substitutions produced chimeras named  
363 YFV-(DENV2) and YFV-(WNV), respectively

364 All primers employed in substitutions, insertions and chimera construction were designed using  
365 NEBaseChanger v1.2.9 software and are listed in Table 1. Single point mutations, insertion of  
366 GLuc and chimera of CBD were introduced into the flavivirus NS1 constructs (DENV, ZIKV, YFV)  
367 using Q5® Site-Directed Mutagenesis Kit (NEB) used according manufacturer's instructions.

368

### 369 **Insertion of flavivirus CBD in the Luciferase reporter**

370 pAc5–mCherry-GLuc-Neo vector designed from a previous work was employed as a template  
371 for chimera construction by the insertion of caveolin binding domain of DENV2 and YFV (13).  
372 The selected region of insertion is located between the secretion signal domain (residues 1-17)  
373 and the luciferase catalytic domain (residues 28-185) (34). DENV2 CBD (FGVFTTNIW) encoded  
374 by sequence TTTGGAGTATTCACCACCAATATATGG, and YFV CBD (TGVFTTRVY) encoded  
375 by sequence ACAGGAGTGTTCCACCACCCGAGTGTAC were introduced between the position  
376 22 and 23 in the GLuc gene using primers designed using NEBaseChanger v1.2.9 software and  
377 primers are listed in Table 1. Insertion of CBD sequences were performed using the Q5® Site-

378 Directed Mutagenesis Kit (NEB). Chimeras of GLuc were named GLuc-(DENV2) for DENV2  
379 inserted sequence and GLuc-(YFV) for YFV inserted sequence.

380 Luciferase activity assay in the supernatants of transfected C6/36 cells with chimeras and wild  
381 type constructions were determined with Pierce™ Gaussia Luciferase Glow Assay Kit (Thermo  
382 Scientific). Percentage of luciferase activity was normalized with DMSO treatment.

### 383 **Cells and plasmid transfection**

384 C6/36 cells from *Aedes albopictus* (ATCC® CRL-1660™) were grown at 28 °C in Eagle's  
385 Minimum Essential Medium (EMEM) (ATCC® 30-2003™), supplemented with 5% fetal bovine  
386 serum (FBS) and 100 U/ml penicillin-streptomycin. Plasmid constructs were transfected into  
387 confluent monolayer of C6/36 cells using lipofectamine reagent Lipofectamine™2000  
388 (Invitrogen). Each 24-well was transfected with 1 µg of plasmid DNA and 2 µL of Lipofectamine.  
389 After 5 h of transfection, cells were added EMEM with a final 10% FBS. After 24h, selective  
390 G418 was added to obtain stable C6/36 cell lines.

### 391 **Reagents and drug treatment**

392 Brefeldin A (BFA) (B6542-Sigma-Aldrich) was dissolved in dimethyl sulfoxide (DMSO, ATCC®).  
393 BFA was used at a concentration of 7 µM in all experiments. Transfected cells were grown in  
394 24-well plates and then, BFA was added to the cells in EMEM 5% FBS and G418 at 500 µg/mL.  
395 Incubation time was 48 hours or kinetic secretion assays at 28°C. After this time, cell  
396 supernatants were collected to measure secreted NS1. In other cases, cells were fixed and  
397 stained for immunofluorescence.

### 398 **Measurement of secreted NS1 protein**

399 The presence of flavivirus NS1 in cell supernatants was measured using a non-commercial, in-  
400 house, ELISA. Briefly, ELISA 96-well plates (Nunc-Immuno™,Sigma-Aldrich®) were coated with  
401 200 ng of purified anti-NS1 monoclonal antibody in carbonate buffer (0.05 M. pH 9.6) and  
402 incubated overnight at 4 °C. Non-specific binding was blocked by incubating with 100 µL/well of  
403 blocking buffer (PBS with 10% fetal bovine serum) for 1 h at 37 °C. At that point, supernatant  
404 samples were added (50 µL/well) and the plate incubated for 1 h at 37 °C. Then, 50 µL/well of  
405 anti-NS1 Mab (kindly donated by Eva Harris, Berkley University, CA) conjugated with biotin for

406 1 h at 37 °C were added, followed by 50 µL/well of streptavidin conjugated with HRP diluted  
407 1:10.000 in PBS incubated for 1h at 37 °C. After each step, wells were washed by rinsing 3x  
408 with washing buffer (PBS with 0.01% Tween 20). The reaction was developed with the addition  
409 of 160 µL/well of TMB (Sigma-Aldrich®) for 15 min and stopped with the addition of 50 µL/well  
410 of 2M H<sub>2</sub>SO<sub>4</sub>. The color development reaction is proportional to amount of secreted NS1. The  
411 amounts of secreted NS1 was estimated in nanograms per mL using serial dilution of  
412 recombinant NS1.

413

#### 414 **Confocal microscopy**

415 Confluent cell monolayers, grown in 24-well plates containing glass coverslips, were transfected  
416 with vectors expressing flavivirus NS1 or GLuc. After the times indicated in the text, cells were  
417 fixed in paraformaldehyde 4% for 10 min. Cells were permeabilized with 0.1% Triton X-100 for  
418 10 minutes at room temperature and stained for DENV-NS1 using anti-NS1 Mab (kindly donated  
419 by Eva Harris, Berkley University, CA), anti-gaussia Luciferase (Pierce PA1181), anti-GRP78  
420 (GTX22902 Genetex), anti-GM130 (G7295 Sigma-Aldrich), anti-CAV-1 (GTX89541 Genetex or  
421 sc-894 Santa Cruz), and Nuclei with DAPI. Anti-mouse Alexa-488 or Alexa-598, anti-goat Alexa-  
422 568 and Anti-rabbit Alexa-647 or Alexa-488 conjugated (Donkey pre-adsorbed, secondary  
423 antibodies, Abcam) were used at 1:800 dilution). Coverslips were mounted in Fluoroshield™  
424 with DAPI (Sigma). Anti-GRP78 and anti-GM130 were used as endoplasmic reticulum and *cis*-  
425 Golgi markers, respectively. The images were analyzed using a LSM 700 confocal microscope.  
426 To evaluate the co-localization between proteins, Pearson correlation coefficients (PCC) were  
427 obtained from at least 20 confocal independent images (laser sections indicated in text) using  
428 the Icy image software and the co-localization studio plugin (35).

#### 429 **Statistical analysis**

430 Values of all assays were expressed as mean ± standard error of three independent  
431 experiments, each in triplicate or indicated in the text. Statistical analyzes were carried out using  
432 the GraphPad Prism version 6.01 software.

433

434 **Author contributions**

435 Conceived and designed the experiments: RRR, JEL

436 Performed the experiments: RRR

437 Analyzed the data: RRR, JEL

438 Contributed reagents and materials: JEL

439 Wrote the paper: RRR, JEL

440

441 **Acknowledgments.** This work was partially funded by CONACYT (Mexico) grant number CB-

442 2015-1 254461 to JEL. Authors declare no conflict of interest.

443

444

445

## References

446 1. Best SM. 2016. Flaviviruses. *Curr Biol* 26:R1258–R1260.

447 2. Guzman MG, Harris E. 2015. Dengue. *Lancet* 385:453–465.

448 3. Bollati M, Alvarez K, Assenberg R, Baronti C, Canard B, Cook S, Coutard B, Decroly E,  
449 de Lamballerie X, Gould EA, Grard G, Grimes JM, Hilgenfeld R, Jansson AM, Malet H,  
450 Mancini EJ, Mastrangelo E, Mattevi A, Milani M, Moureau G, Neyts J, Owens RJ, Ren J,  
451 Selisko B, Speroni S, Steuber H, Stuart DI, Unge T, Bolognesi M. 2010. Structure and  
452 functionality in flavivirus NS-proteins: Perspectives for drug design. *Antiviral Res* 87:125–  
453 148.

454 4. Guzman MG, Kouri G. 2008. Dengue haemorrhagic fever integral hypothesis: confirming  
455 observations, 1987–2007. *Trans R Soc Trop Med Hyg* 102:522–523.

456 5. Acosta EG, Kumar A, Bartenschlager R. 2014. Revisiting Dengue Virus–Host Cell  
457 Interaction, p. 1–109. *In Advances in virus research.*

458 6. Muller DA, Young PR. 2013. The flavivirus NS1 protein: Molecular and structural biology,

- 459 immunology, role in pathogenesis and application as a diagnostic biomarker. *Antiviral Res*  
460 98:192–208.
- 461 7. Akey DL, Brown WC, Jose J, Kuhn RJ, Smith JL. 2015. Structure-guided insights on the  
462 role of NS1 in flavivirus infection. *BioEssays* 37:489–494.
- 463 8. Gutsche I, Coulibaly F, Voss JE, Salmon J, d’Alayer J, Ermonval M, Larquet E, Charneau  
464 P, Krey T, Megret F, Guittet E, Rey FA, Flamand M. 2011. Secreted dengue virus  
465 nonstructural protein NS1 is an atypical barrel-shaped high-density lipoprotein. *Proc Natl*  
466 *Acad Sci* 108:8003–8008.
- 467 9. Beatty PR, Puerta-Guardo H, Killingbeck SS, Glasner DR, Hopkins K, Harris E. 2015.  
468 Dengue virus NS1 triggers endothelial permeability and vascular leak that is prevented by  
469 NS1 vaccination. *Sci Transl Med* 7.
- 470 10. Shi P, Tilgner M, Lo MK, Kent K a, Bernard K a. 2002. Infectious cDNA clone of the  
471 epidemic west nile virus from New York City. *J Virol* 76:5847–56.
- 472 11. Alcalá AC, Palomares LA, Ludert JE. 2018. Secretion of Nonstructural Protein 1 of Dengue  
473 Virus from Infected Mosquito Cells: Facts and Speculations. *J Virol* 92:e00275-18.
- 474 12. Alcalá AC, Hernández-Bravo R, Medina F, Coll DS, Zambrano JL, Del Angel RM, Ludert  
475 JE. 2017. The dengue virus non-structural protein 1 (NS1) is secreted from infected  
476 mosquito cells via a non-classical caveolin-1- dependent pathway. *J Gen Virol* 98:2088–  
477 2099.
- 478 13. Rosales Ramirez R, Ludert JE. 2019. The Dengue Virus Nonstructural Protein 1 (NS1) Is  
479 Secreted from Mosquito Cells in Association with the Intracellular Cholesterol Transporter  
480 Chaperone Caveolin Complex. *J Virol* 93.
- 481 14. Flamand M, Megret F, Mathieu M, Lepault J, Rey FA, Deubel V. 1999. Dengue virus type  
482 1 nonstructural glycoprotein NS1 is secreted from mammalian cells as a soluble hexamer  
483 in a glycosylation-dependent fashion. *J Virol* 73:6104–10.
- 484 15. Byrne DP, Dart C, Rigden DJ. 2012. Evaluating Caveolin Interactions: Do Proteins Interact  
485 with the Caveolin Scaffolding Domain through a Widespread Aromatic Residue-Rich  
486 Motif? *PLoS One* 7:e44879.

- 487 16. Fielding CJ, Fielding PE. 2000. Cholesterol and caveolae: Structural and functional  
488 relationships. *Biochim Biophys Acta - Mol Cell Biol Lipids* 1529:210–222.
- 489 17. Hoop CL, Sivanandam VN, Kodali R, Srnc MN, Van Der Wel PCA. 2011. Structural  
490 Characterization of the Caveolin Scaffolding Domain in Association with Cholesterol-Rich  
491 Membranes.
- 492 18. Akey ADL, Brown WC, Dutta S, Konwerski J, Jose J. 2014. Flavivirus NS1 crystal  
493 structures reveal a surface for membrane association and regions of interaction with the  
494 immune system. *Science (80- )* 343:1–31.
- 495 19. Malavige GN, Ogg GS. 2017. Pathogenesis of vascular leak in dengue virus infection.  
496 *Immunology* 151:261–269.
- 497 20. Chen HR, Lai YC, Yeh TM. 2018. Dengue virus non-structural protein 1: A pathogenic  
498 factor, therapeutic target, and vaccine candidate. *J Biomed Sci. BioMed Central Ltd.*
- 499 21. Liu J, Liu Y, Nie K, Du S, Qiu J, Pang X, Wang P, Cheng G. 2016. Flavivirus NS1 protein  
500 in infected host sera enhances viral acquisition by mosquitoes. *Nat Microbiol* 1.
- 501 22. Nebenführ A, Ritzenthaler C, Robinson DG. 2002. Brefeldin A: Deciphering an enigmatic  
502 inhibitor of secretion. *Plant Physiol.*
- 503 23. Paek SM. 2018. Recent synthesis and discovery of brefeldin a analogs. *Mar Drugs. MDPI*  
504 *AG.*
- 505 24. van der Linden L, van der Schaar HM, Lanke KHW, Neyts J, van Kuppeveld FJM. 2010.  
506 Differential Effects of the Putative GBF1 Inhibitors Golgicide A and AG1478 on Enterovirus  
507 Replication. *J Virol* 84:7535–7542.
- 508 25. Choudhary V, Darwiche R, Gfeller D, Zoete V, Michielin O, Schneiter R. 2014. The  
509 caveolin-binding motif of the pathogen-related yeast protein Pry1, a member of the CAP  
510 protein superfamily, is required for in vivo export of cholesteryl acetate. *J Lipid Res*  
511 55:883–94.
- 512 26. Xu X, Song H, Qi J, Liu Y, Wang H, Su C, Shi Y, Gao GF. 2016. Contribution of intertwined  
513 loop to membrane association revealed by Zika virus full-length NS1 structure. *EMBO J*

- 514 35:2170–2178.
- 515 27. Thomas CM, Smart EJ. 2008. Caveolae structure and function. *J Cell Mol Med* 12:796–  
516 809.
- 517 28. Ricciardi-Jorge T, Bordignon J, Koishi A, Zanluca C, Mosimann AL, Duarte dos Santos  
518 CN. 2017. Development of a quantitative NS1-capture enzyme-linked immunosorbent  
519 assay for early detection of yellow fever virus infection. *Sci Rep* 7:16229.
- 520 29. Youn S, Cho H, Fremont DH, Diamond MS. 2010. A Short N-Terminal Peptide Motif on  
521 Flavivirus Nonstructural Protein NS1 Modulates Cellular Targeting and Immune  
522 Recognition. *J Virol* 84:9516–9532.
- 523 30. Mason PW. 1989. Maturation of Japanese encephalitis virus glycoproteins produced by  
524 infected mammalian and mosquito cells. *Virology* 169:354–364.
- 525 31. González M, Martín-Ruíz I, Jiménez S, Pirone L, Barrio R, Sutherland JD. 2011.  
526 Generation of stable *Drosophila* cell lines using multicistronic vectors. *Sci Rep* 1.
- 527 32. Huynh CQ, Zieler H. 1999. Construction of modular and versatile plasmid vectors for the  
528 high-level expression of single or multiple genes in insects and insect cell lines. *J Mol Biol*  
529 288:13–20.
- 530 33. Qin JY, Zhang L, Clift KL, Huler I, Xiang AP, Ren BZ, Lahn BT. 2010. Systematic  
531 comparison of constitutive promoters and the doxycycline-inducible promoter. *PLoS One*  
532 5:3–6.
- 533 34. Inouye S, Sahara Y. 2008. Identification of two catalytic domains in a luciferase secreted  
534 by the copepod *Gaussia princeps*. *Biochem Biophys Res Commun* 365:96–101.
- 535 35. de Chaumont F, Dallongeville S, Chenouard N, Hervé N, Pop S, Provoost T, Meas-Yedid  
536 V, Pankajakshan P, Lecomte T, Le Montagner Y, Lagache T, Dufour A, Olivo-Marin J-C.  
537 2012. Icy: an open bioimage informatics platform for extended reproducible research. *Nat*  
538 *Methods* 9:690–696.

539

540